

## $^{16}\text{O} + ^{28}\text{Si}$ COUPLED ELASTIC AND INELASTIC SCATTERING NEAR THE BARRIER

M. M. SHALABY<sup>1)</sup>, Cairo

Standard DWBA analyses for inelastic scattering to the  $2^+$ , 1.78 MeV state in  $^{28}\text{Si}$  at  $E_{c.m.} = 21.1$  MeV have been carried out using a weak absorptive optical potential. A satisfactory fit to the data has been obtained only at forward angles. Quantum mechanical coupled-channel calculations satisfactorily account for inelastic scattering cross sections at both forward and backward angles.

### УПРУГОЕ И НЕУПРУГОЕ РАССЕЙНИЕ $^{16}\text{O}$ НА $^{28}\text{Si}$ В СВЯЗАННЫХ КАНАЛАХ ВАЛИЗИ ЭНЕРГЕТИЧЕСКОГО БАРЬЕРА

В работе приводятся результаты стандартного анализа для неупругого рассеяния  $^{16}\text{O}$  на состоянии  $2^+$  ядра  $^{28}\text{Si}$  с энергией 1,78 МэВ при энергии в системе центра масс  $E_{c.m.} = 21,1$  МэВ, используя модель со слабо поглощающими оптическим потенциалом. Удовлетворительное соответствие с экспериментальными данными получено только для углов рассеяния вперед. Квантовомеханические расчеты удовлетворительно объясняют поперечные сечения неупругого рассеяния в связанных каналах как для углов рассеяния вперед, так и для углов рассеяния назад.

### 1. INTRODUCTION

The anomalous large-angle scattering (ALAS) of  $^{16}\text{O} + ^{28}\text{Si}$  has been subject of extensive study. Several different interpretations have been suggested, none of which has proved entirely successful [1]. At  $^{16}\text{O}$  incident energy just above the Coulomb barrier ( $E_{c.m.} = 21.1$  MeV) the experimental angular distribution (for  $\Theta_{c.m.} \approx 100^\circ$ ) has two pronounced oscillations (seven at  $E_{c.m.} = 33$  MeV) which permit their character to be better defined experimentally and lead to more significant optical model fits. For more extensive optical model studies, we refer to the work of Kobos et al. [2], Kahana [3], and Metzaz [4]. The basic ingredient in the real nuclear optical model potential they used is "a rise-dip" kink near the nuclear surface ( $5 \text{ fm} \leq r \leq 8 \text{ fm}$ ). It has been generated by Kobos [2] using a double-folded (M3Y) potential supplemented by a phenomenological model-in-

<sup>1)</sup> Physics Department, Faculty of Science, Ain Shams University, Abbassia — CAIRO, Egypt.

dependent surface correction term, predominantly attractive and appearing to be greatest between 5 fm and 8 fm. Two corrections of surface derivative Woods-Saxon forms were added to a deep (700 MeV) real nuclear potential by Metzaz et al. [4], which, together with their "extremely" transparent imaginary potential, (with a radius of just 1 fm and diffusivity = 0.025 fm) has successfully described ALAS. Kahana et al. [3] take the values of the real nuclear potential  $V(r)$  at prescribed radii between 4 and 8 fm as search parameters in the fitting routine, with constant potential for  $r < 4$  fm and an exponential tail  $e^{-r/a}$  for  $r \geq 8$  fm [3].

In view of the above-mentioned study, we suggest that a conventional optical model potential [5] merits further study, for it reproduces the ALAS and gives a reasonable fit over the whole angular range, particularly at  $E_{c.m.} = 21.1$  MeV. Both real and imaginary parts are of  $W-S$  form, with equal radii and diffuseness, but the absorption is very weak;  $W/V = 0.036$ . This potential was first used in a "standard" DWBA calculation to compare with the measured inelastic scattering cross sections for the  $2^+$ , 1.78 (in  $^{28}\text{Si}$ ) that cover the angular range  $45^\circ - 180^\circ$ . DWBA analyses for quadrupole excitation require different values of Coulomb and nuclear deformation lengths [6, 7, 8, 9], suggesting that inelastic excitation of the  $2^+$ , 1.78 MeV state be treated more accurately via coupled-channel calculations.

### II. METHOD OF ANALYSIS

Quantum mechanical coupled-channel inelastic scattering calculations have been carried out using the code PTOLEMY [10]. For a transition with multipolarity  $L$ , the effective interaction  $H_{Lc}$  contains both nuclear and Coulomb contributions whose radial dependence is

$$H_{Lc} = H_{Lc}^{Nuc}(r) + H_{Lc}^{Coul}(r),$$

with

$$H_{Lc}^{Nuc}(r) = -V_{Lc}^{Nuc} \left[ R_V \frac{dV(r)}{dr} + i R_W \frac{dW(r)}{dr} \right], \quad (2.1)$$

where  $V(r)$  and  $W(r)$  are the real and imaginary part of the optical model potential, and  $V_{Lc}^{Nuc}$  is the nuclear deformation parameter. The radii  $R$ ,  $R'$ ,  $R''$  are the radii of the excited nucleus:

$$R_V = r_V 28^{1/3} \quad \text{and} \quad R_W = r_W 28^{1/3}.$$

The optical model parameters used in the present work are those which successfully fit the elastic scattering data at  $E_{c.m.} = 21.1$  MeV [5]. These parameters are summarized in the following form:

$$V(r) + iW(r) = (38.6 + i1.4) \left\{ 1 + \exp \frac{r - 1.36(16^{1/3} + 28^{1/3})}{0.404} \right\}. \quad (2.2)$$

Since  $R_V = R_W$  here, the real and imaginary potentials have equal deformation lengths.

The Coulomb part of the effective interaction is that derived from the multipole expansion of the potential between a point charge and a uniform charged sphere

$$H_{Lx}^{\text{Coul}}(r_c) = B_{Lx}^{\text{Coul}} R_c' \frac{3ZZ_A e^2}{2Lx+1} \frac{r_c^{Lx}}{R_{Lx+1}^{\text{Coul}}} \quad r < R_c$$

$$r \geq R_c \quad (2.3)$$

$R_c$  is the Coulomb radius of the optical potential  $= r_{oc} (16^{1/3} + 28^{1/3})$ ,  $r_{oc} = 1.0$  fm and  $R_c' = 1.0 (28)^{1/3}$  is the Coulomb radius of the excited  $^{28}\text{Si}$  nucleus. The Coulomb deformation parameter  $B_{Lx}^{\text{Coul}}$  is related to the reduced transition rate  $B(E, L_x, \uparrow)$  by the relation

$$B(E, L_x, \uparrow) = \left[ \frac{3}{4\pi} R_{Lx}^{\text{Coul}} B_{Lx}^{\text{Coul}} \right]^2 \frac{(2J_{\text{final}} + 1)}{(2J_{\text{initial}} + 1)(2L_x + 1)} \quad (2.4)$$

### III. RESULTS AND DISCUSSION

The optical model potential defined by eq. (2) is used as the effective nuclear interaction for the inelastic excitation of the  $2^+$ , 1.78 MeV state in  $^{28}\text{Si}$ . It is this potential (with the appropriate imaginary part) that provided the starting point for the "standard" DWBA inelastic scattering, coupled elastic and coupled-channel inelastic scattering calculations. At any stage of the calculations we stick to the principle that the optical potential to be used should be the elastic potential. This is the reasonable approach to explore how coupling to the first excited  $2^+$  state will affect elastic scattering and to have a consistent description of inelastic scattering cross section in terms of either DWBA or coupled-channel calculations.

#### (a) "Standard" DWBA inelastic scattering

Results of the "standard" DWBA inelastic scattering cross section calculations ( $2^+$ , 1.78 MeV state) are shown in Fig. 1 compared with the corresponding experimental data of Braun-Munzinger et al. [1]. Nuclear and Coulomb interactions used are those defined by equations (2) and (3). For deformation of charge distribution and nuclear matter, values of  $B_2^{\text{Coul}} = -0.407$  and  $B_2^{\text{Nuc}} = -0.337$  were used [11]. The minus sign of  $B_2^{\text{Coul}}$  and  $B_2^{\text{Nuc}}$  is the result of reorientation measurements [12]. As shown in Fig. 1 (dashed line) the quality of fit is quite poor even at the forward angles. DWBA analysis of heavy ion inelastic scattering usually requires that nuclear deformation parameters be considerably smaller than Coulomb deformation parameters [9]. So, we have tried to improve

the fit to the experimental data using  $B_2^{\text{Coul}} = 0.237$  and  $B_2^{\text{Nuc}} = -0.550$ , i. e., allowing a Coulomb deformation length being greater than the nuclear one. Although a considerable improvement has been achieved at forward angles (solid line Fig. 1) the quality of the fit is still by no means acceptable at backward angles ( $\Theta_{c.m.} \geq 120^\circ$ ). It is to be noted that some "not completely standard" DWBA calculation might be useful in order to enlighten the possibilities of the DWBA

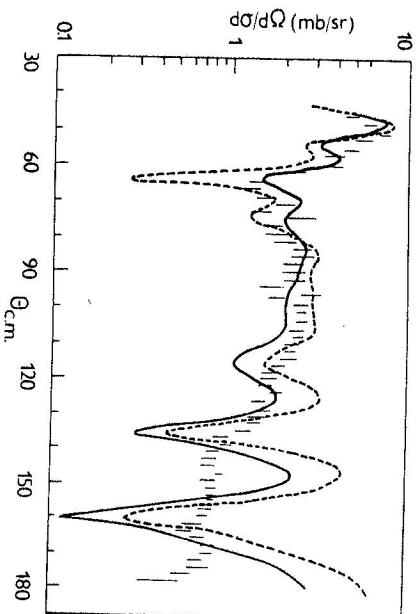


Fig. 1. Differential cross section for the  $^{28}\text{Si}(2^+)$  state at 1.78 MeV. Data are from Braun-Munzinger et al. [1]. Solid and dashed lines are the standard DWBA inelastic scattering calculations using  $B_2^{\text{Nuc}} = -0.237$ ;  $B_2^{\text{Coul}} = -0.55$  and  $B_2^{\text{Nuc}} = -0.337$  and  $B_2^{\text{Coul}} = -0.407$ , respectively.

approach (with varying parameters, including radii, etc.). However, the results of varying deformation parameters (Fig. 1) could be considered as sufficient to represent a clear failure of at least the "standard" collective DWBA methods. Coupled-channel calculations are apparently needed and it is quite reasonable to carry them out with all parameters fixed.

#### (b) Coupled elastic scattering (channel)

To display how coupling to the first excited  $2^+$  state will affect the elastic scattering, the angular distribution of the coupled elastic scattering cross sections (at  $E_{c.m.} = 21.1$  MeV) is shown in Fig. 2a together with the elastic scattering data of Ref. [1]. It is clear that this coupling was sufficient to distort elastic scattering as there is a significant shift in the phase of the oscillatory pattern with respect to the data at angles where the results of the standard optical model potential are in very close agreement to data. Similar results are shown by Dudek et al. [13] in the

coupled-channel analysis of  $^{16}\text{O} + ^{28}\text{Si}$  elastic scattering data (using  $l$ -dependent absorptive potentials) at higher energies  $45 \leq E_{\text{lab}} \leq 63$  MeV. However, in the present analysis no back angle rise in the cross section is observed. A phenomenological theoretical interpretation could be drawn from the character of the coupled elastic reflection coefficients  $|S_l|$  shown in Fig. 2b, compared with the corresponding conventional ones. The pronounced dips in  $|S_l|$  at  $l = 10$  and 13

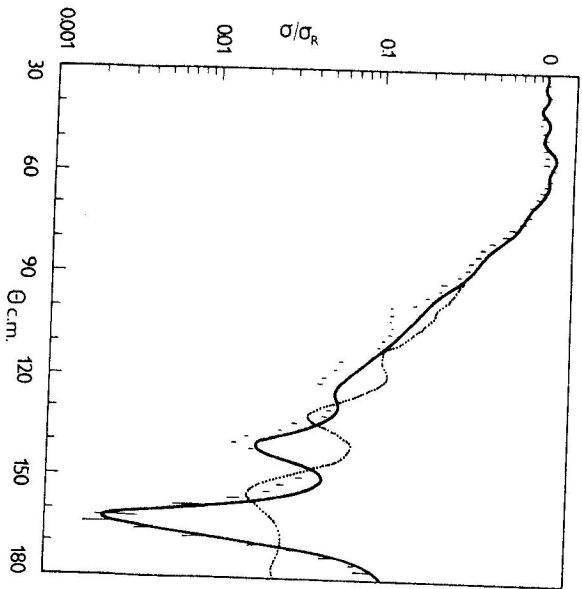


Fig. 2a. Elastic scattering cross section of  $^{16}\text{O} + ^{28}\text{Si}$  at  $E_{\text{cm}} = 21.1$  MeV. Data are from Braun—Munzinger et al. [1]. The solid line is the optical model elastic scattering calculations using potential parameters of Eq. (2). The dotted line is the corresponding coupled elastic scattering calculations.

no longer appear in  $|S_l|$  corresponding to the coupled elastic scattering. Resonances associated with these dips are best seen in the Argand diagram of Fig. 2b, where the resonance circle  $n = 3$  is the largest that does not circulate the origin; other resonances are predominantly elastic as they encircle the origin (McVoy [14]).

### (c) Coupled inelastic scattering (channel)

Results of the coupled-channel inelastic scattering cross sections (using  $B_2^{\text{cul}} = -0.407$  and  $B_2^{\text{cul}} = -0.337$ ) are shown in Fig. (3). The fit to both backward and

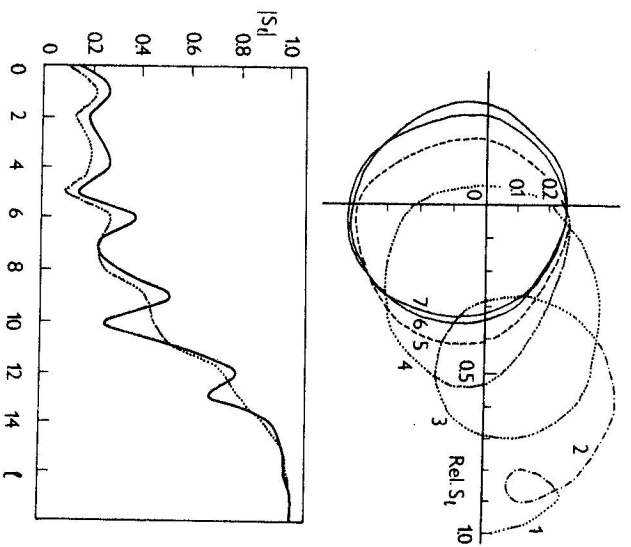


Fig. 2b. A plot of the elastic scattering matrix elements  $S(l)$  in the Argand-Cauchy plane together with the corresponding reflection coefficient  $|S_l|$ .

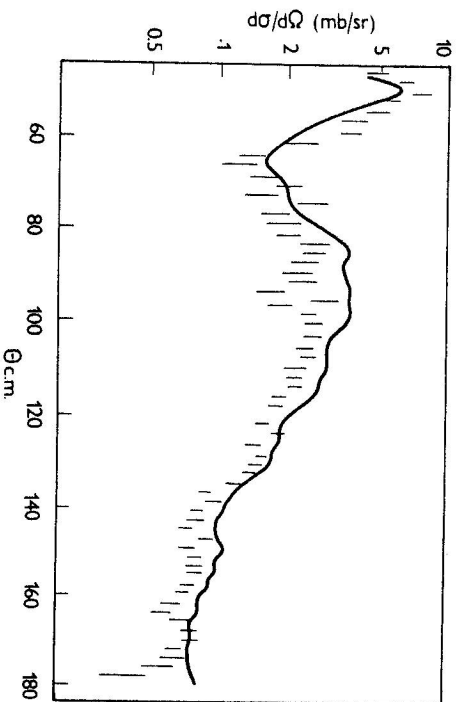


Fig. 3. Coupled-channel inelastic scattering cross sections (to the  $2^+ - 1.78$  MeV state) calculated using  $B_2^{\text{cul}} = -0.407$ ,  $B_2^{\text{cul}} = -0.337$  and potential parameters of Eq. (2).

forward angles is almost satisfactory and shows a considerable improvement relative to that obtained in DWBA calculations. Thus the use of the one channel potential (without changes in its parameters) and the conventional deformation parameters in coupled channel calculations are sufficient to describe the inelastic scattering cross section data. A quantitative interpretation of this could be related to the very weak absorptive character of the potential that avoids the need of any further decrease in the imaginary potential strength (to account for other opened channels) when used in the coupled channel calculations.

#### IV. CONCLUSION

Standard DWBA inelastic scattering calculations, using a weak absorptive optical model potential, are able to produce a satisfactory fit to the data at forward angles, but show a considerable deviation at backward angles ( $\Theta_{c.m.} \geq 120^\circ$ ) even if the Coulomb deformation length is taken greater than the nuclear one. Coupled-channel calculations accomplished this almost satisfactorily at both forward and backward angles. Thus the choice of the one-channel potential to be used in coupled channel analysis is almost straightforward, at least at incident energies close to the Coulomb barrier. This conclusion is of particular interest in the study of sub-barrier fusion cross section enhancement using coupled-channel calculations because the necessary channel potentials may be different from the potential found in one-channel fits [15].

#### ACKNOWLEDGEMENTS

The author is highly indebted to Professor G. R. Satchler for his stimulating suggestions and continuous help and to Professor K. W. McVoy for his kind revision of this manuscript. Also, the author expresses his gratitude for the kind hospitality of both the Physics Division of Oak Ridge National Laboratory and the Physics Department of the University of Wisconsin.

This research was partially sponsored by the Division of High Energy and Nuclear Physics, U. S. Department of Energy, under contract W-7405-eng-26 with the Union Carbide Corporation.

#### REFERENCES

- [1] Braun-Munzinger, P., Barrette, J.: *Phys. Rep.* **87** (1982), 209.
- [2] Kobos, A. M., Satchler, G. R., Mackintosh, R. S.: *Nucl. Phys. A* **395** (1983), 248.
- [3] Kahana, S., Barrette, J., Berthier, B., Chavez, E., Greiner, A., Mermaz, M. C.: *Phys. Rev. C* **28** (1983), 1393.
- [4] Mermaz, M. C., Chavez-Lomeli, E. R., Barrette, J., Berthier, B., Greiner, A.: *Phys. Rev. C* **29** (1984), 147.

- [5] Shalaby, M. El-Naiem, A., Khalil, H., Abdel-Keriem, M.: *Phys. Scr.* **27** (1983), 393.
- [6] Christensen, P. R., Pontopidan, S., Videbaek, F., Bond, P. D., Hansen, O., Thorn, C. E., Levine, M. J., Cheng-Lie, J.: *Phys. Rev. C* **28** (1983), 159.
- [7] Ford, J. L. C., Toth, K. S., Hensley, D. C., Gaedke, R. M., Riley, P. J., Thornton, S. T.: *Phys. Rev. C* **8** (1973), 1912.
- [8] Gross, E. E., Bingham, H. G., Halbert, M. L., Hensley, D. C., Saltmarsh, M. J.: *Phys. Rev. C* **10** (1974), 45.
- [9] Hillis, D. L., Gross, E. E., Hensley, D. C., Bingham, C. R., Backer, F. T., Scott, A.: *Phys. Rev. C* **16** (1977), 1467.
- [10] Rhoades-Brown, M., MacFarlane, M. H., Pieper, S. C.: *Phys. Rev. C* **21** (1980), 2417; *Phys. Rev. C* **21** (1980), 2436.
- [11] Endt, P. M., Van der Leun, C.: *Nucl. Phys. A* **214** (1973), 1.
- [12] Schwalm, D., Bamberger, A., Bizzeiti, P. G., Povh, B., Engelbertink, G. A., Olness, J. W., Warburton, E. K.: *Nucl. Phys. A* **192** (1972), 449.
- [13] Dudek-Ellis, A., Shkolnik, V., Dehnhard, D.: *Phys. Rev. C* **18** (1978), 1039.
- [14] McVoy, K. W.: *Phys. Rev. C* **3** (1971), 1104.
- [15] Stockstand, R. G., Gross, E. E.: *Phys. Rev. C* **23** (1981), 281.

Received August 14 th, 1984

Revised version received October 24 th, 1984